



Electrical conductivity and thermal expansion behavior of MMoO_4 (M = Ca, Sr and Ba)



Binoy Kumar Maji, Hrudananda Jena*, R. Asuvathraman, K.V. Govindan Kutty

Materials Chemistry Division, Chemistry Group, Indira Gandhi Centre for Atomic Research, Kalpakkam 603102, India

ARTICLE INFO

Article history:

Received 11 September 2014
Received in revised form 18 February 2015
Accepted 7 April 2015
Available online 11 April 2015

Keywords:

Inorganic materials
Ionic conduction
X-ray diffraction
Thermal expansion
Chemical synthesis
AC-impedance

ABSTRACT

Alkaline earth (Ca, Sr, Ba) molybdates were synthesized by solid state reaction route. The compounds were characterized by powder-XRD, TG-DTA techniques. The electrical conductivities of these compounds were measured by AC-impedance technique at 673–1073 K. The activation energies of electrical conduction of CaMoO_4 , SrMoO_4 and BaMoO_4 were found to be 1.29 ± 0.01 eV, 1.33 ± 0.01 eV and 1.31 ± 0.01 eV respectively. The linear thermal expansion of these molybdates was measured by dilatometry. The mean coefficients (α_m) of thermal expansion for these compounds were found to be in the range of $9.38 \pm 0.18 \times 10^{-6}$ – $12.96 \pm 0.25 \times 10^{-6} \text{ K}^{-1}$ at 305–1005 K temperature range. The diffusion coefficient (D) values of oxide ion conduction for these molybdates were determined and found to be in the range of $9.48 \pm 0.02 \times 10^{-14}$ – $3.32 \pm 0.01 \times 10^{-10}$ for CaMoO_4 , $5.86 \pm 0.02 \times 10^{-14}$ – $2.50 \pm 0.01 \times 10^{-10}$ for SrMoO_4 and $3.46 \pm 0.02 \times 10^{-14}$ – $1.22 \pm 0.01 \times 10^{-10} \text{ cm}^2 \text{ s}^{-1}$ for BaMoO_4 at 673–1073 K range of temperature.

© 2015 Elsevier B.V. All rights reserved.

1. Introduction

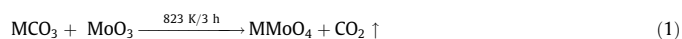
Molybdenum is a very important fission product in thermal and fast reactor fuels [1–3]. Around ~13% of the total fission products produced from U-235 fission are Mo (isotope) [1–3]. Molybdenum found in the form of molybdenum oxide in the irradiated fuel pin and forms various compounds of molybdates under suitable thermodynamic conditions [4]. Alkaline earth molybdates are the most common compounds found in the uranium oxide fuel fission as an interaction product of alkaline earth elements like Sr and Ba (fission product, Sr ~ 5%, Ba ~ 3.4%) with molybdenum oxide. The formation of MMoO_4 (M = Ca, Sr, Ba) compounds in the supercaline-ceramics (a potential waste immobilization matrix) is also known [5–7]. These molybdates form ABO_4 type compounds, where A = Ca, Sr, Ba; B = Mo, W (Scheelite type structure), having tetragonal crystal structure [8,9]. Apart from its relevance to nuclear technology, scheelite type ABO_4 compounds are known to have interstitial oxide ions as the current carriers in their crystal structure [10–13] and can find applications in oxygen sensing devices. The thermodynamic properties of these compounds are well explored by various researchers [14]. The heat capacity values of SrMoO_4 and BaMoO_4 compounds were studied by Singh et al. [14]. But their thermal expansion and electrical properties are not well studied. In the present study, CaMoO_4 , SrMoO_4 and

BaMoO_4 compounds were synthesized by solid state reaction route and characterized by powder-XRD, TG-DTA. The electrical transport properties of these compositions were measured at 673–1073 K and were compared based on electropositive character of Ca, Sr and Ba cations in these compounds. The linear coefficient of thermal expansion of these alkaline earth molybdates was measured by dilatometry. The experimental results obtained on thermal expansion and electrical conductivity is discussed in this paper.

2. Experimental details

2.1. Synthesis and characterization of the powders of CaMoO_4 , SrMoO_4 and BaMoO_4

The preparations of the alkaline earth metal (Ca, Sr and Ba) molybdates were done by solid state reaction route. The stoichiometric amounts of alkaline earth metal carbonates (MCO_3) were mixed with molybdenum oxide (MoO_3) in a mortar–pestle and ground thoroughly to get a homogeneous mixture. Then the mixture was pelleted and heated at 823 K for 3 h in air ambience in a furnace. The product formed was characterized by powder-XRD for phase identification. Philips X'pert Pro MPD, θ – θ system with $\text{Cu K}\alpha$ radiation monochromatized with curved graphite crystal placed in front of the NaI (TI) scintillation detector was used in the step scan mode with a step size of 0.02° for 5 s counting time at each step. M/s. SETARAM-SETSIS-Evolution model was used for recording TG-DTA data at 298–1273 K in air ambient with a heating rate of 5 K/min and cooling rate of 10 K/min. The solid state reaction of the reactants leading to the product is shown in Eq. (1).



* Corresponding author. Tel.: +91 4427480098; fax: +91 4427480065.

E-mail address: hruda66@yahoo.co.in (H. Jena).

(where, M = Ca, Sr and Ba).

The chemical composition of the phase pure compounds was analyzed by ICP-OES and AAS technique and is found to maintain M/Mo mole ratio: 1:1, where M = Ca, Sr, Ba.

2.2. Electrical conductivity measurements of CaMoO_4 , SrMoO_4 and BaMoO_4 pellets

The electrical conductivity measurements on CaMoO_4 , SrMoO_4 and BaMoO_4 were carried out by AC impedance technique. The pellets were prepared in a hydraulic pellet press (Ms. Kimaya Engineers, India) by using a tungsten carbide die and plunger and then the pellets were sintered at 1023–1273 K for 10 h in air ambience. These sintered pellets (around 10 mm dia and 2–3 mm thickness) were used for electrical resistivity measurements. The bottom and top flat surfaces of the pellets were metalized using Ag-paste. The metalized pellets were contacted with Pt-disk shaped electrodes as shown in Fig. 1. The sample, electrodes and thermo-couple assembly is enclosed inside a one end closed alumina tube [15,16]. In this experiment, sample is sandwiched between the two electrodes and firm contact is ensured by tightening the alumina disks with stainless steel nut bolt on both side of the pellet as shown in Fig. 1. The Pt-wires spot welded to the platinum disks were used as leads to measure electrical resistance of the sample at various temperatures. The sample assembly was placed inside the cell and the cell was put inside the furnace well. The temperature of the furnace was controlled by a programmable PID temperature controller with ± 1 K accuracy. The sample temperature was measured with a K-type (chromel–alumel) thermocouple placed at about 2 mm from the sample in the conductivity measurement cell. Resistances of the sample were measured at each 50 K interval. The impedance (Z) measurements were carried out using an Autolab Frequency Response Analyser (FRA) in the frequency range of 100 Hz–1 MHz. The resistance of the samples at various temperatures was determined by fitting the data of $-Z''$ ($Z_{\text{imaginary}}$) vs. Z' (Z_{real}) Nyquist plot using fit and simulate functions available in the Autolab FRA system. The real part of the semicircle ($-Z''$ vs. Z') is taken as the resistance of the sample at a particular temperature. The fitting of the semicircle was done by trial and error method on assuming various equivalent circuit models available with the software provided by Autolab. The equivalent circuit that fits all the points on the semicircle with minimum error is taken as the accepted model and the values of R and C calculated by the model for a particular temperature were taken as the accepted value. The conductivity of the samples was calculated using the formula given in the Eq. (2).

$$\sigma = (L/A) \times (1/R) \quad (2)$$

where L = length of the pellet (cm), A = cross-sectional surface area of the cylindrical pellet (cm^2), R = resistance of the pellet, thereby we got σ in S cm^{-1} . The specific impedance of the samples is calculated by multiplying A/L ratio of the pellet with impedance values ($Z_{\text{im}} = Z''$ or $Z_{\text{re}} = Z'$) at all frequencies and at all temperatures then plotted as ($Z_{\text{im}}/\text{ohm cm}$) vs. ($Z_{\text{re}}/\text{ohm cm}$).

2.3. Thermal expansion measurements of CaMoO_4 , SrMoO_4 and BaMoO_4 pellets

Thermal expansion measurements of CaMoO_4 , SrMoO_4 and BaMoO_4 pellets of around 10 mm dia. and 10 mm height were carried out by dilatometry in the temperature range 298–800 K in air, by using a home-built apparatus [17,18]. Linear Variable Differential Transformer (LVDT) was used as the displacement sensor. The instrument was calibrated by measuring % thermal expansion of known standard single crystal of MgO [19] and ThO_2 pellets [20]. The experimentally measured

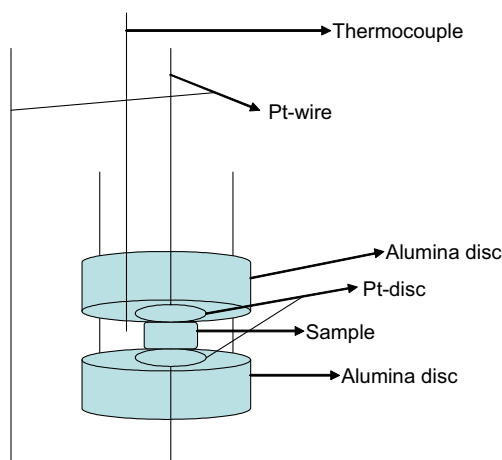


Fig. 1. Schematic of sample pellet and electrode assembly in the high temperature electrical conductivity cell.

value of MgO was interpolated at 2 deg. interval and plotted against temperature. The % thermal expansion was fitted to a polynomial equation of 3rd order. The % expansion obtained at various temperatures by using literature data and experimental data are compared within the measured temperature range. The difference in % thermal expansion reported in the literature (fitted value of equation reported in the literature) and experimentally measured for MgO is added to the experimentally measured value of ThO_2 . The corrected value of ThO_2 is compared with the ThO_2 literature value by Belle and Berman [20]. The following equations (Eqs. (3)–(5)) are used to find out the corrected value of ThO_2 using MgO as the standard.

$$\text{MgO correction value} = \% \text{ expansion of MgO using literature equation} - \% \text{ expansion experimental value of MgO using interpolation} \quad (3)$$

$$\text{MgO corrected \% expansion of ThO}_2 = \text{Experimental \% expansion of ThO}_2 + \text{MgO correction value as given in Eq. (3)} \quad (4)$$

The MgO corrected ThO_2 value is compared with literature value given by Belle and Berman

The literature value and corrected values of ThO_2 are found to be in good agreement. Same procedure is applied to cross check the % thermal expansion of MgO by adding difference of ThO_2 (fitted) and ThO_2 experimental and compared with MgO (literature value/fitted). In this study, the difference in fitted value and experimentally measured value of standard MgO single crystal is taken as the correction factor for the samples studied. The densities and dimensions of the pellets were once again measured after the thermal expansion measurements were complete. The dimensions were found to be unchanged. The percentage of average/mean linear thermal expansion is calculated using Eq. (6).

$$\% \text{ TE} = (\Delta L/L) \times 100 \quad (6)$$

The coefficient of thermal expansion (average CTE = $\alpha_m = \alpha_{av}$) of the compounds was calculated by using the formula given in Eq. (7).

$$\text{Average or mean CTE} = \alpha_m = (\Delta L/L) \times (1/\Delta T) \quad (7)$$

where ΔL = change in length, L is the length of the pellet, ΔT = change in temperature in K.

3. Results and discussions

3.1. Phase identification by powder-XRD

The powder-XRD patterns (Fig. 2) of the compounds confirmed the formation of crystalline single phase alkaline earth metal molybdates (CaMoO_4 , SrMoO_4 and BaMoO_4). There are no reactant phases detected in the XRD pattern of the samples. The XRD patterns of the compounds were indexed by using X-Pert' Pro software and found to stabilize in the tetragonal crystal system (Space Group: $I4_1/a$. (88) Scheelite type structure (ABO_4)). The lattice constants of these compounds were calculated and shown in Table 1. The values determined on indexing the XRD pattern were compared with the literature values [21] and found to agree well

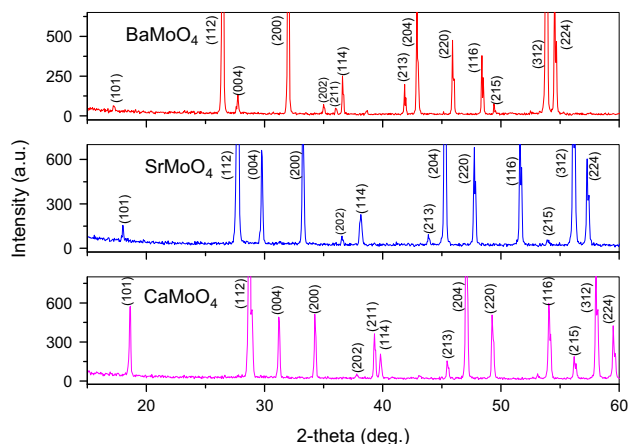
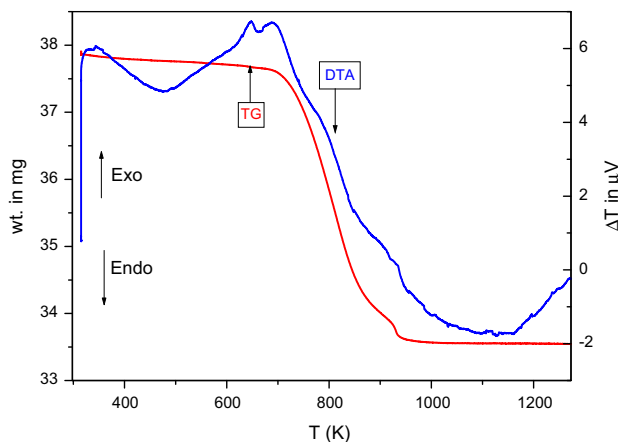
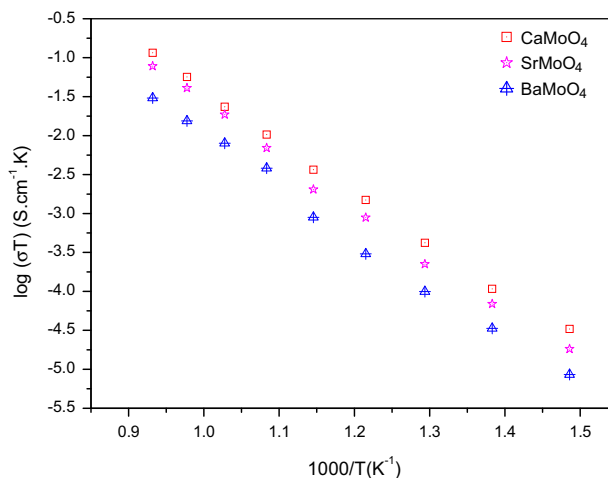
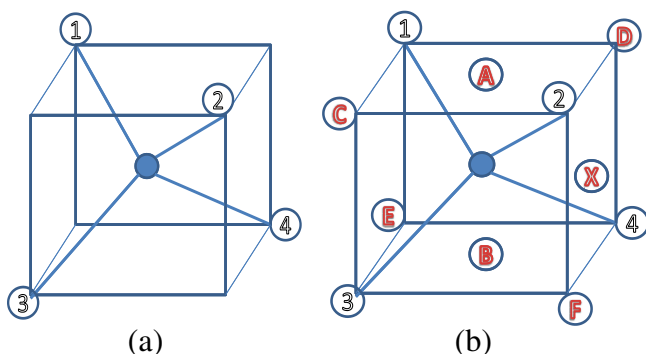


Fig. 2. XRD patterns of CaMoO_4 , SrMoO_4 and BaMoO_4 .

Table 1The lattice constant measurement of CaMoO₄, SrMoO₄ and BaMoO₄ Crystal system: tetragonal, space group: I4₁/a. (88), [21].

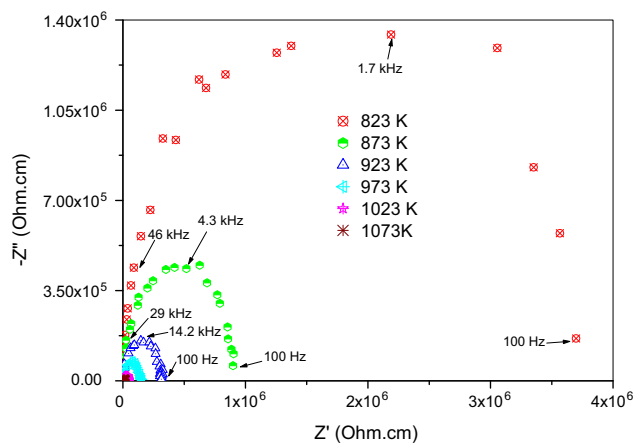
Lattice constants	CaMoO ₄		SrMoO ₄		BaMoO ₄	
	This study	Literature [22]	This study	Literature [23]	This study	Literature [24]
$a = b$ (Å)	5.22 (5)	5.226	5.39 (5)	5.394	5.59 (5)	5.580
c (Å)	11.45 (1)	11.43	12.03 (2)	12.020	12.82 (2)	12.821
$\alpha = \beta = \gamma$ (°)	90		90		90	
V (Å ³)	312.61	312.17	348.91	349.78	400.00	399.23

**Fig. 3.** TG-DTA plot of reaction mixture for BaMoO₄, (to determine the product formation temperature).**Fig. 5.** $\log(\sigma T)$ vs. $1000/T$ (K^{-1}) plots of Ca, Sr and Ba-molybdates.**Fig. 4.** (a) Structure of normal MoO₄²⁻, (b) structure of MoO₄²⁻ containing the interstitial oxygen atoms. A–F and X are the probable positions where the interstitial oxygen atoms exist in the CaMoO₄ crystal structure. Blue filled circles are Mo atoms and hollow circles are O atoms.

with the standard JCPDF patterns PDF card # 29-0351 [22], 08-0482 [23] and 29-0193 [24] for CaMoO₄, SrMoO₄ and BaMoO₄ respectively as shown in Table 1.

3.2. TG-DTA data

The thermal stabilities of the compounds were examined by TG-DTA. A typical TG-DTA plot of the reaction mixture of BaCO₃ and MoO₃ is shown in Fig. 3. A weight loss of 10.5% was observed in the TGA curve. The weight loss is due to the loss of CO₂ from the decomposition of BaCO₃. The broad exotherm centered at ~ 700 K indicates the formation of alkaline earth molybdates with simultaneous weight loss. After the TG-DTA examination carried out at RT – 1273 K in air the sample powder was examined by XRD and found to be phase pure. No other secondary phase was detected in the sample indicating the thermal stability of the samples up to 1273 K in air.

**Fig. 6.** Nyquist plot of CaMoO₄, at indicated temperatures.

3.3. Electrical conductivity data

The electrical conductivity of these compounds was measured by AC-impedance technique. The conductivities were found in the range of 2.11×10^{-8} – 1.08×10^{-4} S cm⁻¹ at the temperature range of 673–1073 K in air ambience. The conductivity of CaMoO₄ measured in this experiment is in good agreement with that of Petrov and Kofstad [11]. The conductivity (σ) was found to show a decreasing trend from CaMoO₄ to BaMoO₄ (i.e. CaMoO₄ > SrMoO₄ > BaMoO₄). The scheelite type structures are known to have interstitial oxide ions in their crystal structure [10,13,25]. The interstitial sites for oxygen atoms are shown in Fig. 4(a) and (b) for CaMoO₄ crystal system. Hence the conductivities are mainly due to the oxide ion migration in these alkaline earth metal molybdates (CaMoO₄, SrMoO₄, and BaMoO₄). The decrease in oxide ion conductivity from CaMoO₄ to BaMoO₄ may

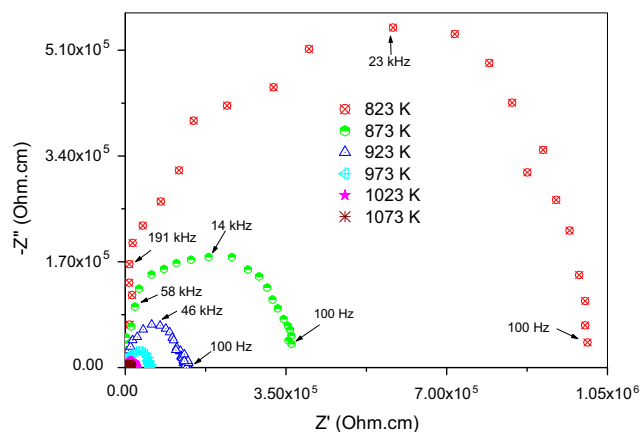


Fig. 7. Nyquist plot of SrMoO₄ at indicated temperatures.

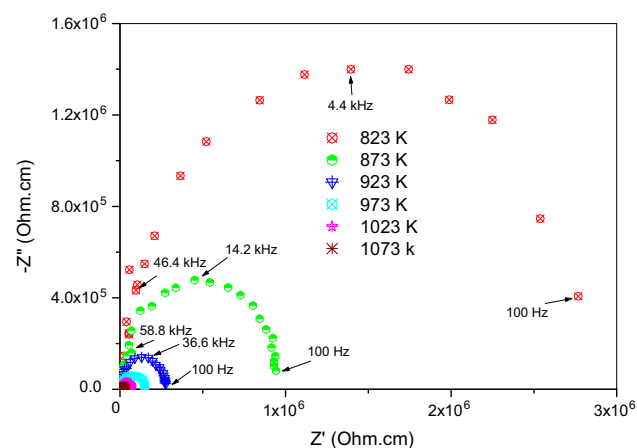


Fig. 8. Nyquist plot of BaMoO₄ at indicated temperatures.

be attributed to the higher electropositive character of Ba²⁺ compared to Sr²⁺ and Ca²⁺; so that the electrostatic attraction of Ba²⁺ on O²⁻ is more, consequently the dragging force is more on oxide ion, hence the mobility/diffusion of O²⁻ is less in BaMoO₄ compared to CaMoO₄.

The activation energies of electrical conduction of these compounds were also evaluated from the $\log(\sigma T)$ vs. $1000/T$ (K) plots (Fig. 5) using Arrhenius equation as given below (Eqs. (8) and (9)).

$$\sigma = (A/T) \exp\left(\frac{-E_a}{k_B T}\right) \quad (8)$$

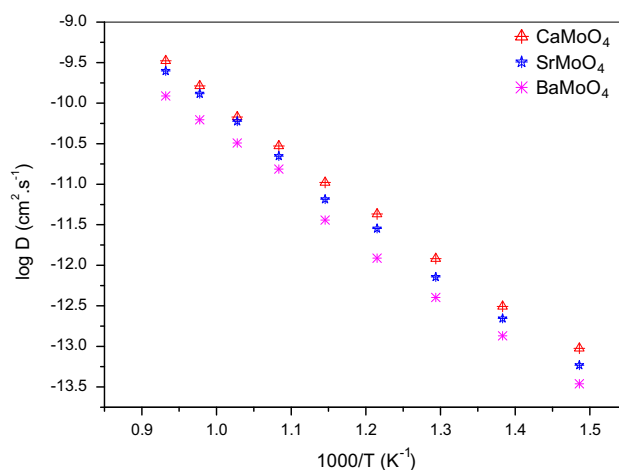


Fig. 10. $\log D$ vs. $1000/T$ plot for CaMoO₄, SrMoO₄ and BaMoO₄.

$$\log(\sigma T) = \log A + \left(\frac{-E_a}{k_B}\right) \times \frac{1}{T} \quad (9)$$

where A = Pre-exponential factor = intercept of the regression fit, k_B = Boltzmann's constant, E_a/k_B = slope of the regression fit, E_a = Activation energy of conduction, T = temperature in K. The slope of the curve is used to calculate the activation energy of conduction. The activation energies for conduction were evaluated by using the above Arrhenius equation. The activation energies were found to be 1.29 ± 0.01 eV for CaMoO₄, 1.33 ± 0.01 eV for SrMoO₄ and 1.31 ± 0.01 eV for BaMoO₄.

Nyquist plots (Z_{im} vs. Z_{re}) of CaMoO₄, SrMoO₄ and BaMoO₄ are given in Figs. 6–8 respectively. The semicircles were fitted using software supplied by Autolab. A typical fitted plot is shown in Fig. 9. The impedance was found to decrease on increasing temperature of measurement (Fig. 6). The semicircle was fitted to an equivalent circuit of R and C in parallel combination. The measured resistance of CaMoO₄ is lower than that of SrMoO₄ and BaMoO₄ at all temperatures. The typical values determined from AC-impedance data at 923 K for CaMoO₄ is $R = 21.9 \pm 3.7$ k Ω and $C = 60.3 \pm 3.4$ pF. However, the R and C values determined for SrMoO₄ and BaMoO₄ are $R = 22.1 \pm 3.7$ k Ω , $C = 64.26 \pm 3.4$ pF and $R = 24.0 \pm 3.7$ k Ω , $C = 58.6 \pm 3.4$ pF respectively. The typical chi-square value for this measurement was 1.3×10^{-3} .

The diffusion coefficient of oxide ion was determined from the electrical conductivity data assuming negligible electronic conduction in these compounds. The diffusion coefficient (D) of O²⁻ in these molybdates was determined by applying Nernst–Einstein equation [26] as given in Eq. (10).

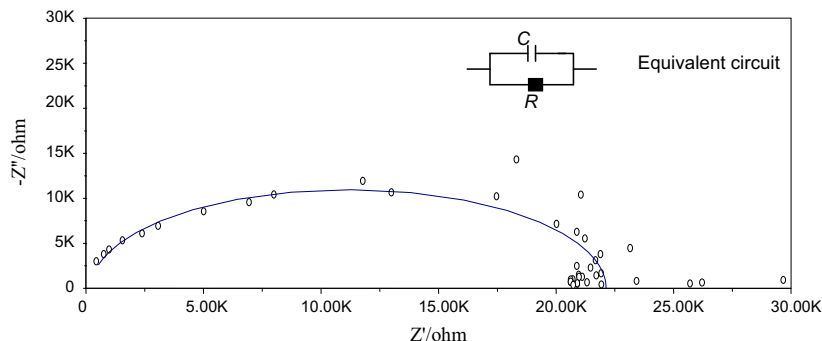


Fig. 9. Fitting of $-Z''$ vs. Z' for CaMoO₄ at 973 K using software supplied by Autolab.

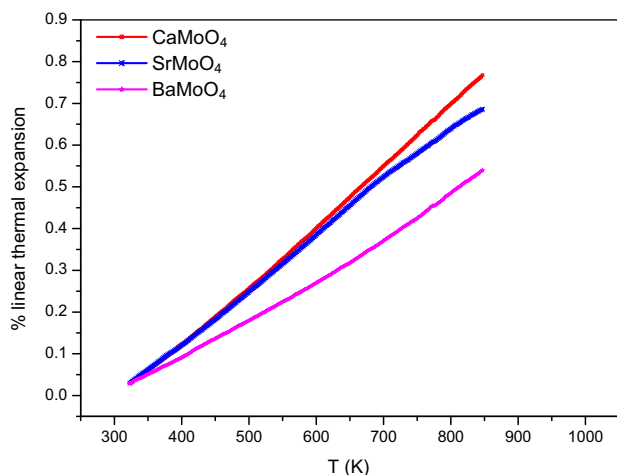


Fig. 11. Percentage thermal expansion vs. temp. (K) plots of CaMoO₄, SrMoO₄ and BaMoO₄.

$$D = k_B T \sigma / n Z^2 e^2 \quad (10)$$

where D = Diffusion coefficient of the current carrying species in $\text{cm}^2 \text{s}^{-1}$, k_B = Boltzmann's constant = $1.380 \times 10^{-23} \text{ J K}^{-1} \text{ mol}^{-1}$, T = Temperature in K, σ = Conductivity in S cm^{-1} , $Z = -2$ for oxide ion, $e = 1.602 \times 10^{-19} \text{ C}$, n = concentration of the current carrying species (oxide ion) in moles per unit volume of the sample (mol cm^{-3}). The diffusion coefficients values of CaMoO₄, SrMoO₄ and BaMoO₄ were plotted $\log D$ vs. $1000/T$ (K^{-1}) in Fig. 10. The diffusion coefficient values were found to be in the range of $9.48 \pm 0.02 \times 10^{-14}$ – $3.32 \pm 0.01 \times 10^{-10}$, $5.86 \pm 0.02 \times 10^{-14}$ – $2.50 \pm 0.01 \times 10^{-10}$ and $3.46 \pm 0.02 \times 10^{-14}$ – $1.22 \pm 0.01 \times 10^{-10} \text{ cm}^2 \text{ s}^{-1}$ in the temperature range of 673–1073 K for CaMoO₄, SrMoO₄ and BaMoO₄ respectively.

3.4. Thermal expansion measurement

The linear thermal expansion of the molybdates was measured by dilatometry. Percentage thermal expansion vs. temperature (K) was shown in Fig. 11. % thermal expansion of BaMoO₄ was found to be the lowest among the three compounds. This may be attributed to relatively stronger bonding among the cation and anion species in the compound compared to SrMoO₄ and CaMoO₄. The thermal expansion coefficient of these molybdates were also calculated and found to be $12.96 \pm 0.25 \times 10^{-6} \text{ K}^{-1}$ (at $T = 313$ – 883 K), $11.39 \pm 0.22 \times 10^{-6} \text{ K}^{-1}$ (at $T = 299$ – 865 K) and $9.38 \pm 0.18 \times 10^{-6} \text{ K}^{-1}$ (at $T = 305$ – 1005 K) for CaMoO₄, SrMoO₄ and BaMoO₄ respectively. The thermal expansion coefficient values of CaMoO₄ calculated by Li et al. [27] are in good agreement with our experimental values. However, they have not reported the thermal expansion behavior of SrMoO₄ and BaMoO₄ compounds. The thermal expansion data on SrMoO₄ and BaMoO₄ are reported for the first time.

4. Conclusion

The electrical conductivities of the alkaline earth molybdates were found to be in the range of 2.11×10^{-8} – $1.08 \times 10^{-4} \text{ S cm}^{-1}$ at the temperature range of 673–1073 K in the air ambience. The decreasing trend in thermal expansion from CaMoO₄ to BaMoO₄ reflects strong bonding character of the solids from CaMoO₄ to BaMoO₄. Further, the decrease in electrical conductivity and

diffusion coefficient of conducting species from CaMoO₄ to BaMoO₄ is due to the increase in electropositive character of Ca²⁺ to Ba²⁺.

Acknowledgements

The authors are grateful to Director, Chemistry group and Director, IGCAR for their constant encouragement and support. The authors acknowledge Mr. Sajal Ghosh, Materials Chemistry Division, Chemistry Group for recording the TG–DTA data of the samples. The authors acknowledge Analytical Chemistry Section/MCD for composition analysis of the samples.

References

- [1] E.A.C. Crouch, Fission products yields from neutron induced fission, *At. Data Nucl. Data Tables* 19 (1977) 417–532.
- [2] I. Sato, T. Nakagiri, T. Hirose, S. Miyahara, T. Namekawa, Fission products release from irradiated FBR MOX fuel during transient condition, *J. Nucl. Sci. Technol.* 40 (2) (2003) 104–113.
- [3] http://en.wikipedia.org/wiki/Nuclear_fission_product. Nuclear_fission_product.
- [4] H. Kleykamp, The chemical state of the fission products in oxide fuels, *J. Nucl. Mater.* 131 (1985) 221–246.
- [5] G.J. McCarthy, High level waste ceramics: materials considerations and product characterization, *Nucl. Technol.* 32 (1977) 92–104.
- [6] G.J. McCarthy, W.B. White, D.E. Pfoertsch, Monazite, *Mater. Res. Bull.* 13 (1978) 1239–1245.
- [7] A.E. Ringwood, S.E. Kesson, K.D. Reeve, D.M. Levins, E.J. Ramm, Synroc, in: W. Lutze, R.C. Ewing (Eds.), *Radioactive Waste Forms for the Future*, Elsevier, Amsterdam, 1988, pp. 223–334.
- [8] R.G. Dickinson, The crystal structures of wulfenite and scheelite, *J. Am. Chem. Soc.* 42 (1) (1920) 85–93.
- [9] V. Thangadurai, C. Knittlmayer, W. Weppner, Metathetic room temperature preparation and characterization of scheelite-type ABO₄ (A = Ca, Sr, Ba, Pb; B = Mo, W) powders, *Mater. Sci. Eng. B* 106 (3) (2004) 228–233.
- [10] Y. Zhang, N.A.W. Holzwarth, R.T. Williams, Electronic band structures of the scheelite materials CaMoO₄, CaWO₄, PbMoO₄, and PbWO₄, *Phys. Rev. B* 57 (20) (1998) 12738–12750.
- [11] A. Petrov, P. Kofstad, Electrical conductivity of CaMoO₄, *J. Solid State Chem.* 30 (1979) 83–88.
- [12] H.N. Im, M.B. Choi, S.Y. Jeon, S.J. Song, Structure, thermal stability and electrical conductivity of CaMoO_{4+d}, *Ceram. Int.* 37 (2011) 49–53.
- [13] T. Esaka, Ionic conduction of scheelite type oxide, *Solid State Ionics* 136 (137) (2000) 1–9.
- [14] Z. Singh, S. Dash, R. Prasad, V. Venugopal, Enthalpy increment measurements of SrMoO₄(s) and BaMoO₄(s), *J. Alloys Comp.* 279 (1998) 287–294.
- [15] H. Jena, K.V.G. Kutty, T.R.N. Kutty, Studies on the structural and ionic transport properties at elevated temperatures of La_{1-x}MnO_{3±δ} synthesized by a wet chemical method, *J. Alloys Comp.* 350 (2003) 102–112.
- [16] Hrudananda Jena, K.V.G. Kutty, T.R.N. Kutty, Proton transport and structural relations in hydroxyl-bearing BaTiO₃ and its doped compositions synthesised by wet-chemical methods, *Mater. Res. Bull.* 39 (2004) 489–511.
- [17] K.V.G. Kutty, R. Asuvathraman, M.V. Krishnaiah, V. Ganesan, R. Parthasarathy, D.S. Subalakshmi, B. Suhasini, K.C. Srinivas, K.A. Gopal, P.V. Kumar, IGC Report No. 283, 2006.
- [18] Hrudananda Jena, R. Asuvathraman, K.V.G. Kutty, P.R. Vasudeva Rao, Comparison of electrical conductivity and thermal properties of borosilicate glass with and without simulated radioactive waste, *J. Therm. Anal. Calorim.* 115 (2014) 367–374.
- [19] E.F. Kaelble, MgO thermal expansion, in: E.F. Kaelble (Ed.), *Handbook of X-rays*, McGraw-Hill, New York, 1967, p. 15 (Chapter 13).
- [20] J. Belle, R.M. Berman, Thorium dioxide: properties and nuclear applications, thermal expansion chapter, in: J. Belle, R.M. Berman (Eds.), *DOE/NE-0060*, US Department of Energy, Govt. Printing Office, Washington DC, 1984, p. 169.
- [21] E. Gürmen, E. Daniels, J.S. King, Crystal structure refinement of SrMoO₄, SrWO₄, CaMoO₄, and BaWO₄ by neutron diffraction technique, *J. Chem. Phys.* 55 (1971) 1093.
- [22] PDF card No. 29-0351, *Natl. Bur. Stand. (U.S.)*, Circ. 539 (6) (1956) 22.
- [23] PDF card No. 08-0482, *Natl. Bur. Stand. (U.S.)*, Circ. 539 (7) (1957) 50.
- [24] PDF card No. 29-0193, *Natl. Bur. Stand. (U.S.)*, Circ. 539 (7) (1957) 7.
- [25] H. Zhao, F. Zhang, X. Guo, Z. Qiren, T. Liu, Ab initio study of electronic structures of BaMoO₄ crystals containing an interstitial oxygen atom, *J. Phys. Chem. Solids* 71 (2010) 1639–1643.
- [26] A. Grandjean, M. Malki, C. Simonnet, Effect of composition on ionic transport in SiO₂–B₂O₃–Na₂O glasses, *J. Non-Cryst. Solids* 32 (2006) 2731–2736.
- [27] H. Li, S. Zhou, S. Zhang, The relationship between the thermal expansions and structures of ABO₄ oxides, *J. Solid State Chem.* 180 (2007) 589–595.